Costratification of a Population of Bipolar Cells With the Direction-Selective Circuitry of the Rabbit Retina

SOLANGE P. BROWN[1]* AND RICHARD H. MASLAND[1,2]
[1]Program in Neuroscience, Harvard Medical School, Boston, Massachusetts 02115
[2]Howard Hughes Medical Institute, Massachusetts General Hospital,
Boston, Massachusetts 02114

ABSTRACT

We have stained a new population of bipolar cells in rabbit retina by using antibodies against the carbohydrate epitope, CD15. The CD15-positive bipolar cells comprise 6–8% of the total cone bipolar cells in peripheral retina. Their axonal and dendritic arbors are similar in size and range from 15 to 50 μm in diameter. The axonal arbors are narrowly stratified in sublamina b of the inner plexiform layer. Double label experiments using an antibody against the calcium binding protein, calbindin, or an antibody against protein kinase C, demonstrate that the CD15-positive bipolar cells are a separate population from the previously identified calbindin-positive cone bipolar cells and the rod bipolar cells. Labeling the processes of starburst amacrine cells with antibodies against choline acetyltransferase showed that the CD15-positive bipolar cells stratify within and slightly more distally to the processes of the ON-starburst amacrine cells. Confocal images of retinal wholemounts showed that the axons of the CD15-positive bipolar cells follow the pattern of the ON-starburst cells' processes. Axonal varicosities of the CD15-positive bipolar cells penetrate the bundles formed by the processes of the ON-starburst cells. This finding suggests that the CD15-positive bipolar cell provides input to the ON-starburst amacrine cells and/or the ON-plexus of the ON-OFF direction-selective ganglion cells. J. Comp. Neurol. 408:97–106, 1999.   © 1999 Wiley-Liss, Inc.

Indexing terms: CD15; cholinergic amacrine cell; ganglion cell; cell adhesion molecule; inner plexiform layer; immunoreactivity; PKC

Mammalian retinas contain rod bipolar cells, which exclusively contact rods and form a homogeneous population of neurons, and cone bipolar cells, which contact cones. Unlike the rod bipolar cells, the cone bipolar cells can be further subdivided. Recent studies in rat and monkey have identified nine types of cone bipolar cells based largely on the stratification of the cells' axonal processes in the inner plexiform layer (IPL; Boycott and Wässle, 1991; Euler and Wässle, 1995). In the cat, five types of bipolar cells stratifying in sublamina b of the IPL were identified (Cohen and Sterling, 1990).

The morphologies of bipolar cells suggest that each type interacts with a subset of other retinal neurons because the processes of the different amacrine and ganglion cells also ramify in specific layers within the IPL. This likely reflects functional differences among bipolar cells, because neuronal processes within the IPL are segregated based on their function. For example, the processes of retinal cells that respond to light OFF ramify in sublamina a of the IPL, whereas the processes of cells that respond to light ON ramify in sublamina b (Famiglietti and Kolb, 1976; Nelson et al., 1978).

Further specialization within the two major sublaminae of the IPL exists. One specialized ganglion cell of the rabbit retina is the ON-OFF direction-selective (DS) ganglion cell (Barlow and Levick, 1965). This cell responds selectively to stimuli moving in one direction. This cell's dendritic arbor is bistratified: one portion narrowly stratifies within sublamina a of the IPL, whereas the other ramifies narrowly within sublamina b (Amthor et al., 1984, 1989; Yang and Masland, 1994). The processes of two types of amacrine cells, the ON- and OFF-starburst cells, ramify narrowly in the same layers of the IPL as the dendrites of ON-OFF DS

ganglion cells (Famiglietti, 1981, 1983, 1992). The processes of the two cells cofasciculate (Vaney et al., 1989), and starburst cells synapse upon ON-OFF DS ganglion cells (Famiglietti, 1991, 1992). Synapses from cone bipolar cells onto both starburst and ON-OFF DS ganglion cells have been seen by electron microscopy (Famiglietti, 1983, 1985, 1991; Brandon, 1987). In rat, GLT-1 bipolar cells stratify above and below (but not within) the level of the processes of the ON-starburst cells (Brandstätter et al., 1995). To date, no well-characterized population of cells except for the starburst amacrine cells has been identified as contacting the ON-OFF DS ganglion cell (Famiglietti, 1983, 1985, 1991, 1992; Brandon, 1987; Young and Vaney, 1991; Mills and Massey, 1992; Massey and Mills, 1996; Massey and Zhang, 1998).

CD15, a carbohydrate epitope (3-fucosyl-N-lactosamine), is expressed by a variety of cell types, including cells in the central nervous system and the immune system (Lasky, 1992; Springer, 1994; Gocht et al., 1996). A previous study demonstrated that in some mammalian retinas, several neuronal types are immunopositive for CD15 although no specific populations were identified (Andressen and Mai, 1997). We have further characterized the distribution of this antigen in the rabbit retina. A subset of bipolar cells was selectively labeled with antibodies against CD15. Double label experiments compared the newly identified CD15-positive bipolar cell with the other known populations of bipolar cells in the rabbit. The level of axonal stratification of the CD15-positive bipolar cell suggested that it might ramify at the same level as the processes of ON-starburst amacrine cells and ON-OFF DS ganglion cells. Double label experiments confirmed this hypothesis and suggest that CD15-positive bipolar cells play a role in the ON-OFF DS neuronal circuitry.

MATERIALS AND METHODS

New Zealand rabbits, ranging from 290 g to 3.5 kg, were deeply anesthetized with ketamine (100 mg/kg) and xylazine (20 mg/kg). An 0.5% solution of proparacaine was applied topically to the orbit. After enucleation, rabbits were euthanized with anesthetic in accordance with institutional guidelines. All protocols were approved by the Subcommittee on Research Animal Care of the Massachusetts General Hospital.

The globe was hemisected, the vitreous was removed, and the retina was isolated in Ames medium (Sigma, St. Louis, MO) as previously described (Yang and Masland, 1994). The isolated retina was fixed for 1 hour in 4% formaldehyde (Ted Pella, Redding, CA) in ice-cold 0.1 M phosphate buffer (PB), pH 7.4, and then rinsed for several hours in 0.1 M PB.

Wholemounts were first incubated in 4% normal donkey or goat serum with 0.5% Triton X-100 in 0.1 M PB overnight. The tissue was then incubated in primary antibody in the same solution for 1–4 days at room temperature or 4°C. When using the anti-CD15 antibody derived from the hybridoma (see below), we used the supernatant directly with 4% normal serum and 0.5% Triton X-100 added. When processing the tissue with the supernatant, 0.2–0.002% sodium azide was occasionally added. When the complete cell culture medium alone was used as a negative control, there was no staining. To visualize the staining, immunofluorescent secondary antibodies (1:50–1:100) were used to stain the retinas over-

night after several washes in 0.1 M PB. If the wholemount was being double labeled, the process was repeated for the second antigen. Alternatively, a biotinylated secondary antibody was used. The wholemount was rinsed several times in 0.1 M PB and then incubated in ABC solution (Vectastain Elite ABC Kit, Vector Laboratories, Burlingame, CA) overnight. Diaminobenzidine (DAB) with nickel/cobalt intensification was used to visualize the staining (Adams, 1981).

For vibratome sections, small pieces of retina were embedded in 4% agar in 0.1 M PB and sections were cut at 40–50 µm. Sections were preincubated for 2 hours in 4% normal donkey or goat serum with 0.3% Triton X-100 in 0.1 M PB. The sections were then incubated overnight with the primary antibody in the same solution or in the supernatant with 4% normal serum and 0.3% Triton X-100. To visualize the staining, the sections were incubated for 2 hours with the secondary antibody in the same solution. The process was repeated for double labels. All staining was performed at room temperature or at 4°C with constant agitation. Both sections and whole-mounts were mounted in Vectashield (Vector Laboratories, Burlingame, CA) to reduce fading of the fluorescent labels. DAB material was mounted in 75% glycerol.

The mouse monoclonal antibody against CD15 was obtained from the hybridoma cell line MMA (HB 78, American Type Culture Collection, Manassas,VA). A purified antibody against CD15 (Becton Dickinson, San Jose, CA) derived from the same hybridoma line was also used at dilutions of 5–20 µg/ml. No difference could be detected between the purified antibody from Becton Dickinson and the culture supernatant produced in-house. The rabbit polyclonal antibody against calbindin (Swant, Bellinzona, Switzerland) was used at a dilution of 1:10,000. It stains the same population of bipolar cells as the mouse monoclonal antibody against calbindin (Sigma) used by Massey and Mills (1996; data not shown). A rabbit polycolonal antibody against recoverin, a gift of K.W. Koch (Forschungszentrum Jülich GmbH, Germany), stained the calbindin-positive bipolar cells as well as bipolar cells whose axons ramified in sublamina a of the IPL and were clearly not the CD15-positive bipolar cell (data not shown; Massey and Mills, 1996). The goat polyclonal anti-choline acetyltransferase (Chemicon, Temecula, CA) was used at a dilution of 1:20–100. The rabbit polyclonal antibody against protein kinase C (Chemicon) was used at a dilution of 1:1,000.

To avoid cross-talk between the fluorochromes during confocal microscopy, the majority of double labels were done using fluorescein isothiocynate (FITC) and indodicarbocyanine (CY5). Rhodamine was sometimes substituted for CY5. All secondary antibodies were obtained from Jackson Immunoresearch Laboratories (West Grove, PA) and Vector Laboratories and were used at dilutions of 1:50–1:100. When labeling multiple antigens, all secondary antibodies used were from the same host (goat or donkey) and were selected for their minimal cross-reactivity with the other species of primary antibodies used.

All fluorescent specimens were viewed using a Biorad MRC-1024 confocal microscope equipped with a krypton-argon laser (Hercules, CA). The following laser lines and emission filters were used: FITC: 488 nm and 522 DF32 nm; rhodamine: 568 nm and 605 DF32 nm; and CY5: 647 and 680 DF32 nm, respectively. The DAB material was viewed using an Axioplan microscope (Carl Zeiss, Thorn-
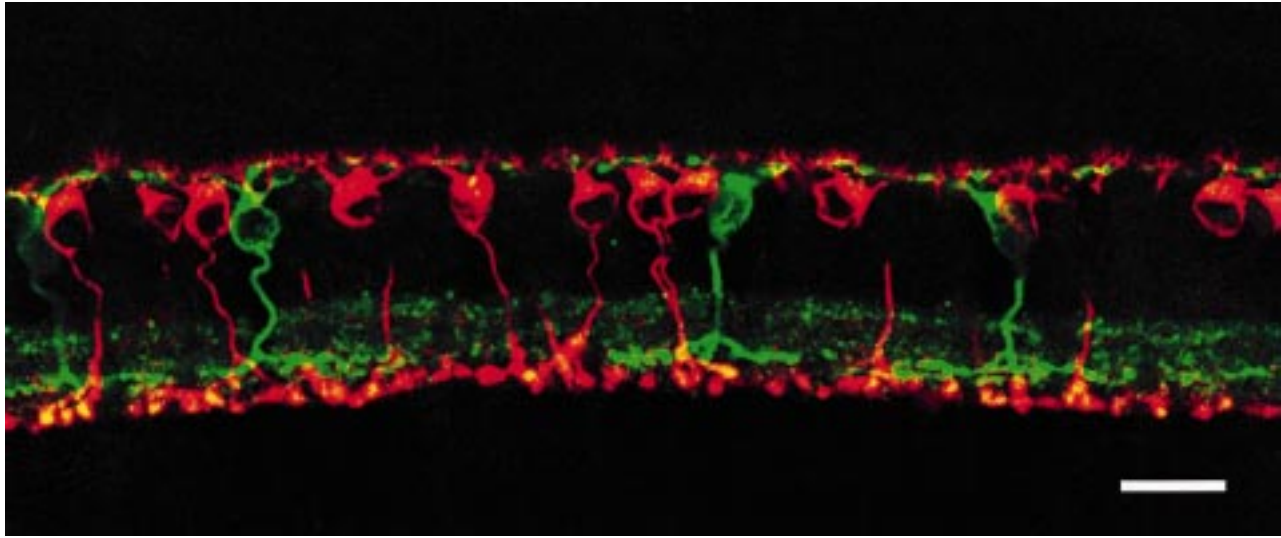
Fig. 1. Vertical section double labeled with antibodies against protein kinase C (PKC) and against the carbohydrate epitope, CD15. The photoreceptor side is up in the micrograph. This confocal image of a vibratome section shows the CD15-positive bipolar cells (green) labeled with antibodies against CD15. The rod bipolar cells (red) were labeled with antibodies to PKC. Yellow regions most prominent in the rod bipolar cell terminals and somas indicate that the rod bipolar cells are also weakly immunopositive for CD15. This rabbit weighed 575 g. Scale bar = 25 μm.

wood, NY) and was photographed using TMax 100 and Ektachrome Elite II 200 (Kodak, Rochester, NY). The brightness and contrast of images were adjusted using Adobe Photoshop (ver. 4.0.1). No other digital processing was carried out.

RESULTS

Anti-CD15 antibody labeled rod bipolar cells weakly and another type of bipolar cell brightly. Figure 1 shows a vertical section of the rabbit retina double labeled with an antibody against protein kinase C (PKC), visualized as red, and the antibody against CD15, visualized as green. Two distinct populations of cells are labeled. As has been previously shown, antibodies against PKC label the rod bipolar cells (Negishi et al., 1988; Young and Vaney, 1991). The yellow staining, visible at spots within the rod bipolar cell terminals, indicates that the rod bipolar cells are also weakly immunopositive for CD15.

A second population of cells, green in Figure 1, is brightly labeled with antibodies against CD15. The dendrites of these cells can clearly be seen among the dendritic processes of the rod bipolar cells. The cell bodies of the CD15-positive bipolar cells are located in the outermost portion of the inner nuclear layer (INL). However, their somas are slightly more proximal than the cell bodies of the rod bipolar cells. This characteristic is most evident in wholemount preparations, where the CD15-positive cell bodies come into focus more proximally than the somas of the rod bipolar cells. After traversing most of the IPL, the axonal stalk usually branches a few microns before descending to its final level of stratification. However, the majority of the axonal processes of the CD15-positive cells are narrowly stratified within sublamina b of the IPL. The prominent varicosities along the axonal processes are clearly visible. They sometimes can be seen to dip below the bulk of the axonal arborization.

In addition to these bipolar cells, the antibody also lightly labeled three broad bands in the IPL. In rare instances (not shown in the figures), bipolar cells with axonal processes terminating in the outer one-third of the IPL were labeled with the CD15 antibody. The staining in the outer portion of the IPL may therefore represent puncta of CD15-positivity within the axonal processes of these rarely stained cells. In a few sections, rare amacrine cells whose processes descended deep into the IPL were also labeled with the antibody to CD15.

In retinas of adult rabbits, the anti-CD15 antibodies revealed the complete morphology, including the axonal and dendritic processes, of only a small number of bipolar cells. Because CD15 has been shown to be developmentally regulated elsewhere in the nervous system (Gocht et al., 1996), we suspected that the incomplete staining might be due to the down-regulation of the antigen during development. We therefore used retinas of rabbits 3–8 weeks in age for the majority of our studies. (These retinas have reached adult physiology and morphology; Masland, 1977; McArdle et al., 1977.) In these animals, a greater number of CD15-positive bipolar cells was completely labeled, and all the figures are from animals weighing 400–600 g. Other than the intensity of cells labeled, we found no systematic differences in the labeling among the retinas.

Because of this staining pattern, isolated CD15-positive bipolar cells were easily found in wholemount preparations, with separately visible dendritic and axonal arbors. Figure 2 shows an example of the dendritic and axonal arbors of such a cell. The dendritic processes are thin and contain apparent specializations, often occurring at the tip of a dendritic branch. The individual axonal processes of the CD15-positive bipolar cells are more robust than the slender dendritic processes. Typically, three or four branches depart from the axonal stalk and often branch further. Varicosities are located throughout the axonal arbor and these often come into focus slightly more proxi-
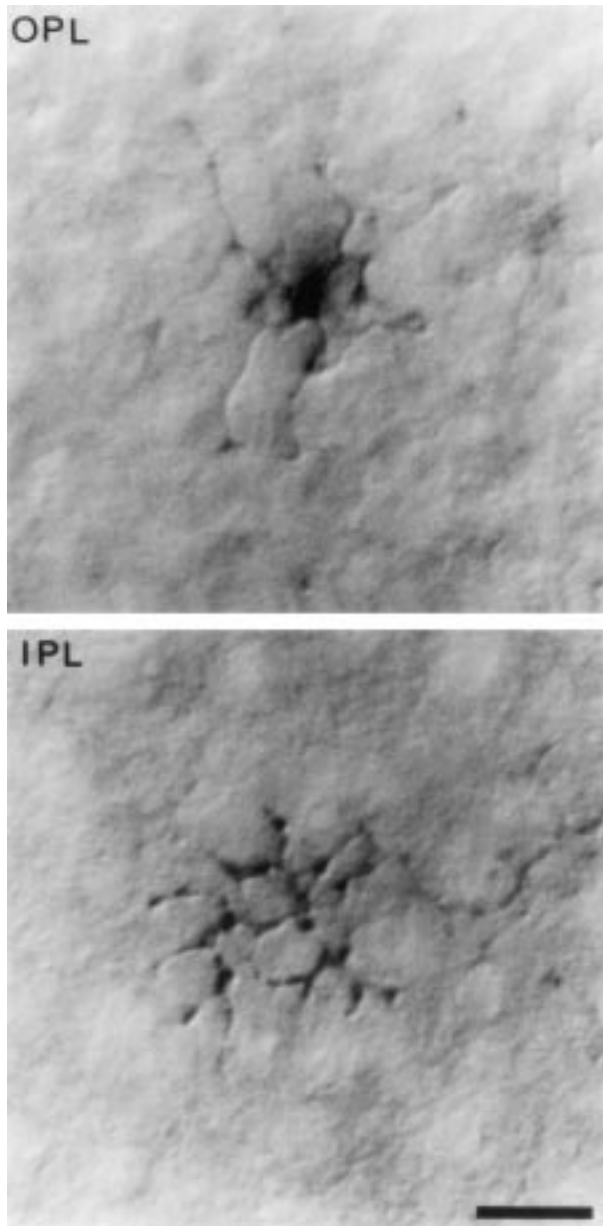
Fig. 2.   Wholemount view of an isolated CD15-positive bipolar cell, visualized with diaminobenzidine (DAB). Focus in the outer plexiform layer (OPL): the fine dendrites of this cell often terminate with an apparent specialization. Focus in the inner plexiform layer (IPL): the axon is studded with varicosities. These are in focus here, whereas the majority of the axonal arbor is slightly out of focus; the varicosities protrude more vitreally than the majority of the axonal processes. This cell was located 10 mm ventral to the optic nerve. Scale bar = 10 µm.

mally than the bulk of the axonal processes. (Other examples can be seen in Fig. 4).

Using antibodies against the calcium binding protein, calbindin, Massey and Mills (1996) have described a cone bipolar cell that also narrowly stratifies in sublamina b of the IPL, just distal to the rod bipolar cell terminals. To explore the relationship between this cell and the CD15-positive cell, double label experiments with antibodies against calbindin and CD15 were performed. As can be seen in Figure 3A–C, the CD15-positive bipolar cell (green)
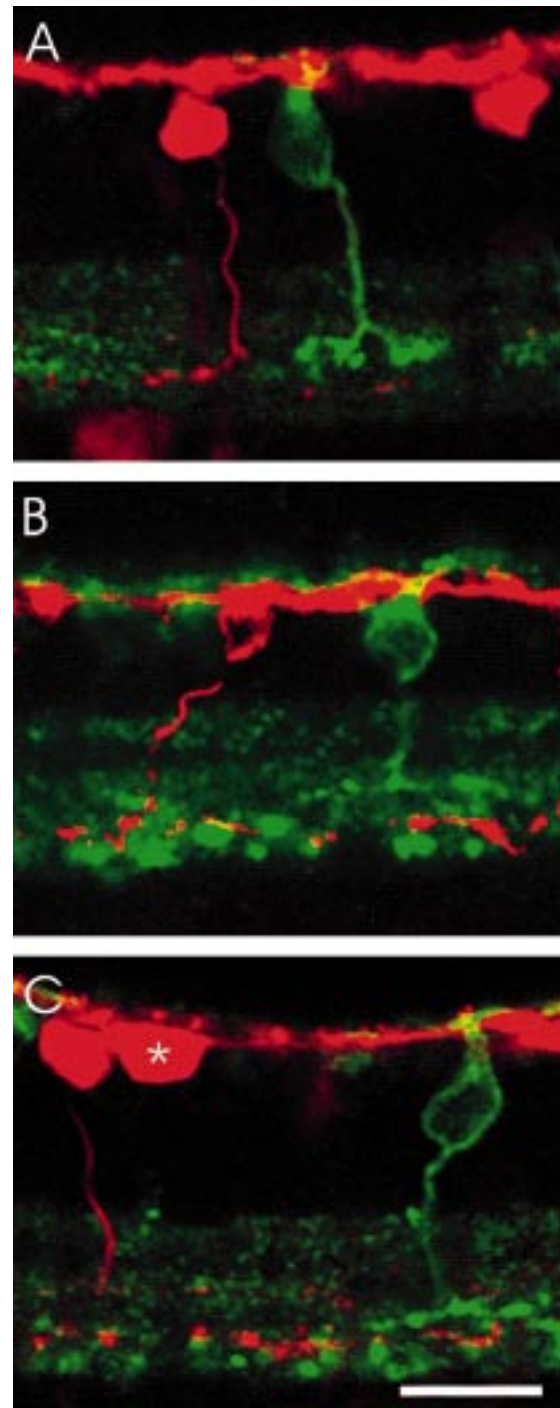

Fig. 3.   **A–C:** Vertical sections double labeled with antibodies against CD15 (green) and against calbindin (red). These confocal images demonstrate that the CD15-positive bipolar cells are distinct from the calbindin bipolar cell previously identified (Massey and Mills, 1996). The axons of the calbindin-positive bipolar cells (red) ramify between the axons of the CD15-positive bipolar cells (green) and the rod bipolar terminals (green). In no case was a bipolar cell double labeled. The only yellow seen is in the outer plexiform layer (OPL), where the dendrites of the two cell types cross; it is not indicative of colocalization of the two antigens. Horizontal cells are also stained with antibodies against calbindin (asterisk in C). Scale bar = 25 µm.

is clearly different from the calbindin-positive cone bipolar cell (red). In no case was a bipolar cell double labeled with both antibodies. Some rare amacrine cells were double labeled with both antibodies to calbindin and to CD15 (data not shown), providing a positive control for the double label methodology by showing that we were capable of visualizing double labeling should it occur.

The axonal arborizations of the calbindin-positive bipolar cells narrowly stratify between the axonal arborizations of the CD15-positive bipolar cells and the rod bipolar cell terminals (Fig. 3B,C). There are also subtle morphological differences in their axonal endings. The CD15-positive axons are studded with prominent varicosities. Furthermore, as stained by these antibodies, the axonal arbors of the CD15-positive bipolar cells appear more robust than the long and slender axonal processes of the calbindin-positive bipolar cells. Finally, the stouter axons of the CD15-positive bipolar cells appear to cover the retina more densely in wholemount preparations than the axonal arbors of the calbindin-positive bipolar cells.

The mosaic of those CD15-positive bipolar cells that are completely stained, including the dendrites, soma, and axon, at first seems incomplete, as can be seen in Figure 4D: the brightly labeled axonal arbors do not tile the retina completely. However, in the INL, the CD15-positive somas form a population of regularly distributed cells (Fig. 4A). The intensity of staining of the somas was variable. At one extreme are cells with only the soma dimly labeled. At the other are cells with very bright somas; these are the cells whose axons and dendrites are clearly visible, as in Figure 4B–E. Although we cannot entirely rule out the possibility that some other cells were inadvertently included or that unstained members of the population went uncounted, we believe that these somas represent the population of CD15-positive bipolar cells. The rare amacrine and OFF bipolar cells labeled with antibodies to CD15 had somas located closer to the IPL than the somas of the CD15-positive bipolar cells and were therefore in a different plane of focus when viewing the wholemount preparations. A nearest neighbor analysis (Wässle and Riemann, 1978) of the CD15-positive cells confirms that the CD15-positive bipolar cells are nonrandomly distributed within the INL (Fig. 5A).

In some fortuitous locations, several nearby cells were fully labeled. In these cases, the processes of the CD15-positive bipolar cells appear to tile the retina (Fig. 4B, C, and E). In no case did labeled axonal arbors appear to significantly overlap. The density of CD15-positive somas and the area of the stained axonal arbors of CD15-positive bipolar cells at that eccentricity predict a coverage factor of approximately one; in other words, every point in visual space is sampled by approximately one of the CD15-positive bipolar cells. For example, at a position 9 mm ventral to the optic nerve (V9), the density of CD15-positive cells is 546 cells/mm^2 (n = 4 retinas). By dividing the area by the number of cells, one calculates that the average axonal or dendritic diameter should be approximately 48 µm to achieve a coverage of one. As can be seen in Figure 4B and C, these representative cells located at V9 have axonal and dendritic diameters of approximately 40–50 µm.

By double labeling wholemount preparations with antibodies against CD15 and against PKC, we counted the CD15-positive cells as well as the rod bipolar cells at several retinal locations. As shown in Figure 5B (open circles), the absolute density of the CD15-positive bipolar cells decreases with increasing eccentricity, as would be expected. However, because of deformation during processing, the apparent absolute density of any retinal cell can vary significantly, particularly with the thicker and mechanically softer retinas of young rabbits used for most of these studies. A more informative number than absolute density is the ratio of a new cell to a known retinal neuron, because it controls for variations introduced during tissue processing. As can be seen in Figure 5B (black circles), the ratio of CD15-positive bipolar cells to rod bipolar cells is constant across eccentricities. The apparent increase in absolute density at V12 is most likely artifactual, because the ratio of CD15-positive bipolar cells to rod bipolar cells remains unchanged. Figure 5C shows the ratio of CD15-positive bipolar cells to rod bipolar cells at a position 9 mm ventral to the optic nerve in four retinas from four different rabbits. Again, this ratio is similar across all four rabbits.

These data indicate that there are 4–5 rod bipolar cells for every CD15-positive bipolar cell. Strettoi and Masland (1995) counted all the bipolar cells in representative regions of the retina, as well as the fraction accounted for by rod bipolar cells. Using simple arithmetic, our results combined with their data indicate that the CD15-positive bipolar cells comprise 6–8% of the total cone bipolar cells of the peripheral rabbit retina. This percentage is very similar to the values calculated for the other known narrow-field bipolar cells in rabbit, the DAPI-Ba1 bipolar cell (7–8%), the DAPI-Ba2 bipolar cell (6–10%), and the calbindin-positive bipolar cell (7–9%; Mills and Massey, 1992; Strettoi and Masland, 1995; Massey and Mills, 1996).

Comparison with the processes of starburst amacrine cells

The location of the axonal processes of the CD15-positive bipolar cells suggested that the cells might stratify near the processes of the ON-cholinergic amacrine cells in the rabbit retina (the ON-starburst cells). Furthermore, previous double label experiments indicated that the calbindin-positive bipolar cell stratified just proximal to the processes of the ON-starburst amacrine cells (Massey and Mills, 1996). We therefore performed double label experiments with antibodies against choline acetyltransferase (ChAT), which label the cholinergic or starburst amacrine cells, and antibodies against CD15. As seen in the confocal images of vertical sections in Figure 6A and B, when the processes of starburst amacrine cells were labeled with anti-ChAT, the axonal arborizations of the CD15-positive bipolar cells were found to stratify narrowly within and slightly above the ON-starburst processes. The CD15-positive axonal processes seemed to lie above the ChAT-positive band with small knobs dipping down into the ChAT-positive band.

In wholemount preparations double labeled with antibodies against CD15 and antibodies against ChAT, the axons of the CD15-positive bipolar cells can be seen to loosely follow the pattern of the ChAT-positive processes of the ON-starburst amacrine cells (Fig. 6C, D). In other words, the axonal processes of the CD15-positive bipolar are located preferentially over the processes of the ON-starburst cells and avoid the "holes" interspersed among the bundles of ChAT-positive processes (Tauchi and Masland, 1985; Brandon, 1987; Vaney et al., 1989). However, unlike the dendrites of the ON-OFF DS ganglion
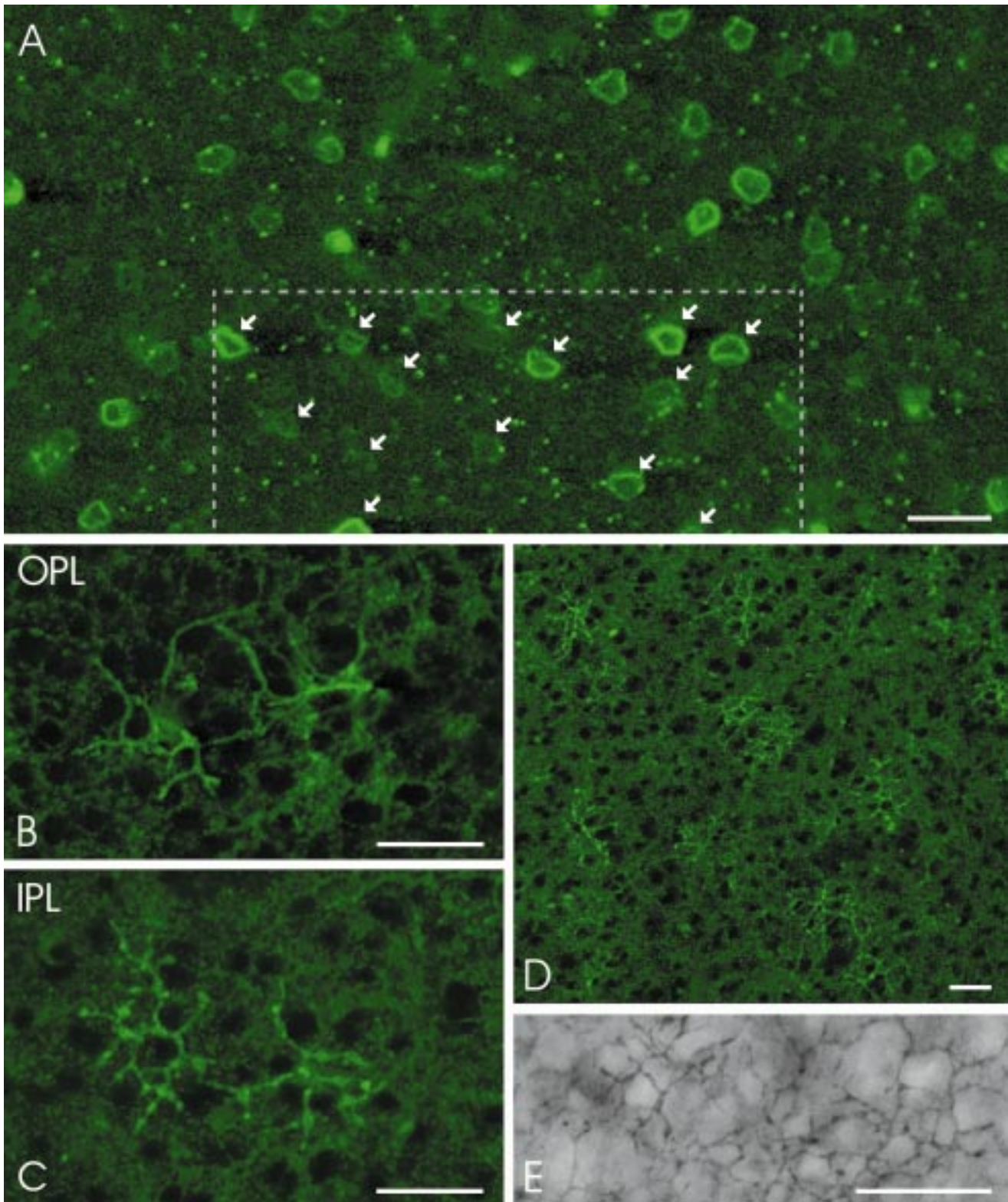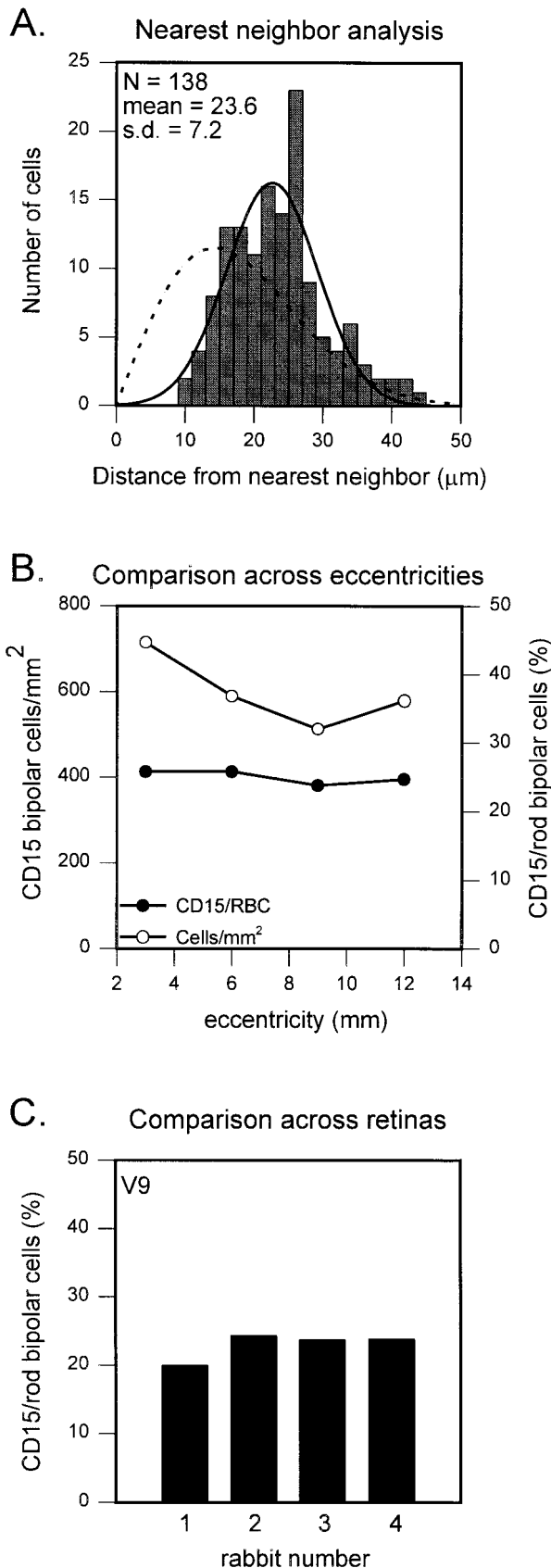
Fig. 4. Wholemount views of the population of CD15-positive cells. **A:** A confocal image of the inner nuclear layer (INL) at a region 6 mm ventral to the optic nerve. The CD15-positive somas form a regular mosaic within the INL. Within the rectangle (dashed lines), all the CD15-positive somas are indicated by arrows. (Cells contacting the upper and rightmost borders are excluded.) The somas are labeled with a variety of intensities by the antibodies against CD15. **B** and **C:** Confocal images of a pair of CD15-positive bipolar cells located 9 mm ventral to the optic nerve head. With the focus in the outer plexiform layer (OPL; B), the dendritic processes of the two neighboring cells tile the retina without significant overlap. Likewise, with the focus in the inner plexiform layer (IPL; C), the axonal systems of these two cells appear closely opposed without significant overlap. **D:** Confocal image of the axonal processes of a number of CD15-positive bipolar cells located 10 mm ventral to the optic nerve head. The incomplete staining of the mosaic of brightly labeled axons can be appreciated. The variation corresponds to the varying intensity with which the somas are labeled. **E:** Photomicrograph of the axonal processes of CD15-positive bipolar cells in the far periphery. In areas where the complete mosaic of axonal processes appeared well-labeled, they had a continuous honeycombed appearance. Scale bars = 25 μm.

A.

Nearest neighbor analysis

N = 138
mean = 23.6
s.d. = 7.2

(y-axis: Number of cells; x-axis: Distance from nearest neighbor (μm))

B.

Comparison across eccentricities

(left y-axis: CD15 bipolar cells/mm^2; right y-axis: CD15/rod bipolar cells (%); x-axis: eccentricity (mm))

● CD15/RBC
○ Cells/mm^2

C.

Comparison across retinas

V9

(y-axis: CD15/rod bipolar cells (%); x-axis: rabbit number)

cells, the axonal processes of the CD15-positive bipolar cells do not cofasciculate with the starburst processes. As can be seen in Figure 6C and D, the varicosities of the CD15-positive bipolar cells are located more proximally than the bulk of the axonal processes. Hence, the general arrangement consists of axonal processes approximately aligned with the ChAT-positive processes and with isolated varicosities penetrating the bundles of ChAT-positive processes.

The inset to Figure 6C illustrates this point at higher magnification: one can see two small holes in the bundle of ChAT-positive processes that are filled in with two CD15-positive varicosities. This inset clarifies why the CD15-positive processes appear discontinuous in Figure 6C and 6D: the varicosities penetrating the ON-ChAT band are emphasized at this plane of focus. In Figure 6E, with the focus slightly more distal to the ON-ChAT band, one can see the continuity of the CD15-positive axons. The general pattern of the ChAT-positive bands is reflected in the CD15-positive axonal processes at this level (notice the absence of processes in the large "hole" located centrally in the figure). These results suggest that the CD15-positive bipolar cells make contacts with ON-starburst amacrine cells. Because the dendrites of the ON-OFF DS cells cofasciculate with the starburst processes (Vaney et al., 1989), it is equally possible that the CD15-positive bipolar cells provide input to the ON-plexus of ON-OFF DS ganglion cells' dendritic arbors.

DISCUSSION

Using antibodies to the carbohydrate epitope, CD15, we have identified a population of brightly labeled rabbit bipolar cells. Our results demonstrate that: (1) the CD15-positive bipolar cells form a separate population from the rod bipolar cells as shown by double label experiments with antibodies against PKC; (2) the CD15-positive bipolar cell is also distinct from the only previously identified ON-cone bipolar cell in rabbit, as shown by double label experiments with antibodies against calbindin; (3) there are 4–5 rod bipolar cells for every CD15-positive bipolar cell. Hence, these cells make up 6–8% of the cone bipolar cells in rabbit retina; (4) the CD15-positive bipolar cell stratifies deep in the IPL. The axonal processes of the calbindin-positive cone bipolar cells are sandwiched between the axonal arbors of the CD15-positive bipolar cells

Fig. 5. Analysis of the population of CD15-positive bipolar cells. **A:** Nearest neighbor analysis (Wässle and Riemann, 1978) of the CD15-positive bipolar cells. The histogram shows the distances from each cell body to its nearest neighbor. The nearest neighbor histogram can be approximated by a Gaussian curve (solid line). The dotted line represents the distribution for a similar field with the same density but of randomly distributed cells. These data indicate that the CD15-positive bipolar cells form a regular mosaic. The field used for the analysis was located 9 mm ventral to the optic nerve head. **B:** Distribution of CD15-positive bipolar cells across eccentricities. The open circles indicate the absolute density of CD15-positive bipolar cells in one retina. The density decreases from central retina to the periphery. The ratio of CD15-positive bipolar cells to PKC-positive rod bipolar cells (RBC) is indicated by the black circles. This ratio remains constant across all eccentricities. The apparent increase in absolute density seen at the extreme periphery is most likely due to deformation because the ratio of the two cells is constant even at this eccentricity. **C:** The ratio of CD15-positive bipolar cells to rod bipolar cells is shown for 4 retinas at a distance of 9 mm ventral to the optic nerve head. The ratio is similar across the 4 individuals, averaging 23%.
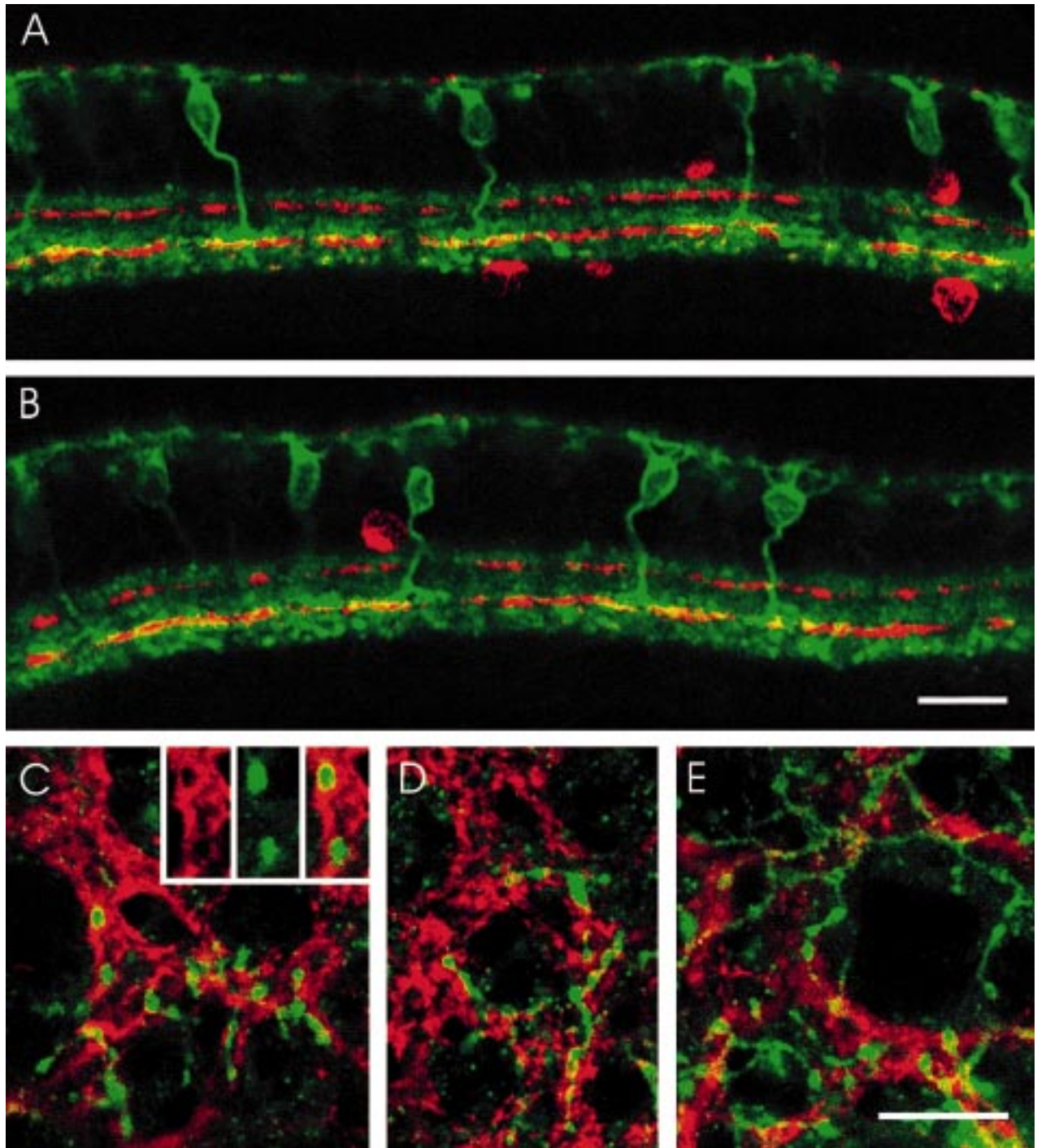
Fig. 6. Vertical sections and wholemounts double labeled with antibodies against CD15 and against choline acetyltransferase (ChAT). The CD15 (green) was visualized using fluorescein isothiocynate (FITC), whereas the ChAT (red) was visualized using indodicarbocya-nine (CY5). **A** and **B:** In these confocal images of vertical sections, the axons of the CD15-positive bipolar cells can be observed to ramify above and within the ChAT-positive band created by the processes of the ON-starburst amacrine cells. Places where the CD15-positive axons overlap with the starburst processes appear yellow. Some rod bipolar cell terminals can be seen below the ChAT band in sublamina b. Some nonspecific ChAT staining was sometimes seen in the outer plexiform layer (OPL). **C–E:** In these confocal images of retinal wholemounts, the pattern formed by the processes of the ON-starburst cells is revealed with antibodies against ChAT (red). As can be seen in C and D, the axonal varicosities of the CD15-positive bipolar cells (green) follow the same pattern as the ChAT-positive processes. The **inset** in C shows how the varicosities penetrate the bundles of ChAT-positive processes. In the leftmost panel of the inset, two small holes in the bundle of ChAT-positive processes can be seen. The isolated CD15-positive varicosities, shown in the central panel of the inset, fit into these holes when the two images are superimposed (rightmost panel of the inset). In E, the focus is located slightly distally to the ChAT-positive processes, which are just slightly out of focus; this makes the continuity of the CD15-positive axons easier to appreciate. Even at this focal plane, one can see that the CD15-positive processes are nonrandomly positioned: they tend to align with the mosaic of the starburst processes. These images were taken at 8, 6, and 9 mm ventral to the optic nerve. Scale bars = 25 μm for A and B; 10 μm for C–E.

and the rod bipolar cell terminals; and (5) the axonal processes of the CD15-positive bipolar cells stratify within and slightly above the ChAT-positive band produced by the processes of the ON-starburst cell.

Comparison with other bipolar cells in the rabbit

Previous studies have identified five populations of narrow-field bipolar cells in rabbit retina (Young and Vaney, 1991; Mills and Massey, 1992; Massey and Mills, 1996). The axonal processes of three of these cells, the DAPI-Ba1, DAPI-Ba2, and the DAPI-Ba3 bipolar cells (Mills and Massey, 1992), ramify in the OFF sublamina of the IPL and are thus definitively separate from the CD15-positive bipolar cell. The results presented here demonstrate that the CD15-positive bipolar cell is also distinct from both the calbindin-positive bipolar cell (Massey and Mills, 1996) and the rod bipolar cell (Young and Vaney, 1991). Finally, the size of the axonal and dendritic arbors of the CD15-positive cell distinguish it from the known wide-field bipolar cells in rabbit (Famiglietti, 1981; Jeon and Masland, 1995). Using the Golgi method, Famiglietti (1981) identified two narrow-field bipolar cells with axonal terminals ramifying in sublamina b of the IPL (nb1 and nb2). Although it is difficult to compare the two preparations, Famiglietti's drawings indicate that the CD15-positive bipolar cell is much more narrowly stratified than either of those cells.

The CD15-positive bipolar cell represents 6–8% of the total cone bipolar cells and approximately 5% of all bipolar cells in rabbit retina, a value similar to three other known populations of narrow-field cone bipolar cells (Mills and Massey, 1992; Strettoi and Masland, 1995; Massey and Mills, 1996). Combining these data, one can make a rough calculation of the bipolar cells that remain unaccounted for. In the midperiphery, rod bipolar cells account for 20–25% of all bipolar cells (Strettoi and Masland, 1995). The five known populations of cone bipolar cells represent another 20–30% of the total bipolar cells (CD15: 5%; DAPI-Ba1: 5–6%, DAPI-Ba2: 6–7%, DAPI-Ba3: 2–3%, Mills and Massey, 1992; calbindin: 4–6%, Massey and Mills, 1996). The rare wide-field bipolar cells are numerically insignificant (Jeon and Masland, 1995). Thus roughly 45–60% of bipolar cells remain to be studied as populations in the rabbit retina. The remaining populations of cone bipolar cells are similarly large in the rat and monkey (Kouyama and Marshak, 1992; Grünert et al., 1994; Euler and Wässle, 1995).

Function of the CD15-positive bipolar cell

Because of the level of stratification of its axons, the CD15-positive bipolar is almost certainly an ON-cone bipolar cell. Furthermore, it may well provide input to the direction-selective circuitry of the retina. Previous studies using electron microscopy have shown that both the ON-OFF DS ganglion cell and the ON-starburst cell receive bipolar cell input (Famiglietti, 1983, 1985, 1991; Brandon, 1987). The CD15-positive bipolar cell would be a strong candidate for providing input to either of these cells. In fact, the geometry produced by cofasciculation of the starburst processes and ON-OFF DS ganglion cell dendrites makes it quite plausible that a bipolar cell like this one could provide excitatory input to both cells. As the processes of the DAPI-3 amacrine cell costratify with the starburst amacrine cells and the ON-OFF DS ganglion

cells, the CD15-positive bipolar cells may also provide input to these cells (Wright et al., 1997). One assumes that a similar bipolar cell provides input to the OFF-starburst cells and the OFF-plexus of the ON-OFF DS ganglion cells and DAPI-3 cells. (However, it is unlikely to be the rare CD15-positive OFF bipolar cell, as its axons seem to ramify above the OFF-starburst processes.) Although the precise level of stratification of the dendrites of the ON DS ganglion cell relative to the ON-starburst cells is still unclear (Famiglietti, 1992; Kittila and Massey, 1997a), the CD15-positive bipolar cell may provide input to these cells as well. Studies of the synaptic connections of the CD15-positive bipolar cells at the level of the electron microscope are necessary to confirm any of these predictions.

Although much discussion has centered around the possibility that the directional computation occurs at the level of the ON-OFF DS ganglion cell, there is no evidence against and some evidence for the possibility that the computation occurs presynaptically, i.e., by presynaptic inhibition of the axon terminal of the bipolar cell (Ariel and Daw, 1982; Famiglietti, 1991, 1993; Vaney, 1991; Borg-Graham, 1992; Borg-Graham and Grzywacz, 1992; Amthor and Grzywacz, 1993; Grzywacz et al., 1997; He and Masland, 1997). Furthermore, although starburst amacrine cells provide significant input onto ON-OFF DS ganglion cells (Famiglietti, 1991, 1992), ON-OFF DS cells retain their direction selectivity after the starburst cells have been selectively killed or their excitatory output is blocked by cholinergic antagonists (Ariel and Daw, 1982; Kittila and Massey, 1997b; He and Masland, 1997). In experiments exploring the effects of glutamate, the neurotransmitter of bipolar cells, on direction selectivity, particular classes of glutamate receptors have been implicated in the mechanism for direction selectivity (Linn and Massey, 1992; Cohen and Miller, 1995). Therefore, as has often been suggested previously, an alternative possibility is that stimulus motion in the null direction would produce inhibition on bipolar axon terminals via an inhibitory amacrine cell. In that case, the axon terminal of the CD15-positive bipolar cell (and its OFF counterpart) could be the site of the inhibition that causes direction selectivity.

Role of CD15 in the retina

CD15 may be involved in cell-cell adhesion, either in a homophilic fashion or as a ligand for a receptor such as a member of the selectin family of cell adhesion molecules (Lasky, 1992; Springer, 1994; Gocht et al., 1996). Several neuronal types are weakly immunopositive for CD15 in the mammalian retina (Andressen and Mai, 1997). However, that a putative cell-cell adhesion molecule is strongly expressed in one of the candidate cells of the direction-selective circuit in rabbit suggests further studies exploring the overall biological role of CD15 in the retina, and molecules of the immune system generally. Although the role of CD15 in the immune system is defined (Lasky, 1992; Springer, 1994), its functions in the nervous system are less clear. The retina, with its well-defined structure, would be a favorable tissue for further work. If CD15 is playing a role in cell-cell adhesion, it would be interesting to see what a lack of CD15 would do to the retinal circuitry. It would also be useful to identify the receptor for this ligand in the retina and the type of cell that expresses it. In addition to a possible role in cell-cell adhesion and migration, CD15 could have other functions in the retina. For

example, cell-cell adhesion molecules have recently been implicated in synaptic plasticity (for example, see Fields and Kouichi, 1996). It is conceivable, though highly speculative, that such plasticity is necessary for the creation, during development, of the DS circuitry.

LITERATURE CITED

Adams JC. 1981. Heavy metal intensification of DAB-based HRP reaction product. J Histochem Cytochem 29:775.

Amthor FR, Grzywacz NM. 1993. Directional selectivity in vertebrate retinal ganglion cells. In: Miles FA, Wallman J, editors. Visual motion and its role in the stabilization of gaze. Amsterdam: Elsevier. p 79–100.

Amthor FR, Oyster CW, Takahashi ES. 1984. Morphology of on-off direction-selective ganglion cells in the rabbit retina. Brain Res 298:187–190.

Amthor FR, Takahashi ES, Oyster CW. 1989. Morphologies of rabbit retinal ganglion cells with complex receptive fields. J Comp Neurol 280:97–121.

Andressen C, Mai JK. 1997. Localization of the CD15 carbohydrate epitope in the vertebrate retina. Vis Neurosci 14:253–262.

Ariel M, Daw NW. 1982. Pharmacological analysis of directionally sensitive rabbit retinal ganglion cells. J Physiol 324:161–185.

Barlow HB, Levick WR. 1965. The mechanism of directionally selective units in rabbit's retina. J Physiol (Lond) 178:477–504.

Borg-Graham LJ. 1992. On directional selectivity in vertebrate retina: an experimental and computational study. MIT Artificial Intelligence Laboratory. AI Technical Report No. 1350. Cambridge, MA.

Borg-Graham LJ, Grzywacz NM. 1992. A model of the directional selectivity circuit in retina: transformations by neurons singly and in concert. In: McKenna T, Davis J, Zornetzer SF, editors. Single neuron computation. New York: Academic Press. p 347–375.

Boycott BB, Wässle H. 1991. Morphological classification of bipolar cells of the primate retina. Euro J Neurosci 3:1069–1088.

Brandon C. 1987. Cholinergic neurons in the rabbit retina: dendritic branching and ultrastructural connectivity. Brain Res 426:119–130.

Brandstätter JH, Greferath U, Euler T, Wässle H. 1995. Co-stratification of GABA$_A$ receptors with the directionally selective circuitry of the rat retina. Vis Neurosci 12:345–358.

Cohen E, Sterling P. 1990. Demonstration of cell types among cone bipolar neurons of cat retina. Phil Trans R Soc Lond B 330:305–321.

Cohen ED, Miller RF. 1995. Quinoxalines block the mechanism of directional selectivity in ganglion cells of the rabbit retina. PNAS 92:1127–1131.

Euler T, Wässle H. 1995. Immunocytochemical identification of cone bipolar cells in the rat retina. J Comp Neurol 361:461–478.

Famiglietti EV. 1981. Functional architecture of cone bipolar cells in mammalian retina. Vision Res 21:1559–1563.

Famiglietti EV. 1983. ON and OFF pathways through amacrine cells in mammalian retina: the synaptic connections of "starburst" amacrine cells. Vision Res 23:1265–1279.

Famiglietti EV. 1985. Synaptic organization of ON-OFF directionally selective ganglion cells in rabbit retina. Soc Neurosci Abstr 11:337.

Famiglietti EV. 1991. Synaptic organization of starburst amacrine cells in rabbit retina: analysis of serial thin sections by electron microscopy and graphic reconstruction. J Comp Neurol 309:40–70.

Famiglietti EV. 1992. Dendritic co-stratification of ON and ON-OFF directionally selective ganglion cells with starburst amacrine cells in rabbit retina. J Comp Neurol 324:322–335.

Famiglietti EV. 1993. A 'bilayer' model of directional selectivity in rabbit retina. IOVS 34:985.

Famiglietti EV, Kolb H. 1976. Structural basis for ON- and OFF-center responses in retinal ganglion cells. Science 194:193–195.

Fields RD, Kouichi I. 1996. Neural cell adhesion molecules in activity-dependent development and synaptic plasticity. Trends Neurosci 19:473–480.

Gocht A, Struckhoff G, Löhler J.1996. CD15-containing glycoconjugates in the central nervous system. Histol Histopathol 11:1007–1028.

Grünert U, Martin PR, Wässle H. 1994. Immunocytochemical analysis of bipolar cells in the macaque retina. J Comp Neurol 348:607–627.

Grzywacz NM, Tootle JS, Amthor FR. 1997. Is the input to a GABAergic or cholinergic synapse the sole asymmetry in rabbit's retinal directional selectivity? Vis Neurosci 14:39–54.

He S, Masland RH.1997. Retinal direction selectivity after targeted laser ablation of starburst amacrine cells. Nature 389:378–382.

Jeon C-J, Masland RH. 1995. A population of wide-field bipolar cells in the rabbit's retina. J Comp Neurol 360:403–412.

Kittila CA, Massey SC. 1997a. Confocal imaging of ON-OFF directionally selective and putative MTN-projecting ganglion cells in rabbit retina. IOVS 38:S949.

Kittila CA, Massey SC. 1997b. Pharmacology of directionally selective ganglion cells in the rabbit retina. J Neurophys 77:675–689.

Kouyama N, Marshak DW. 1992. Bipolar cells specific for blue cones in the macaque retina. J Neurosci 12:1233–1252.

Lasky LA. 1992. Selectins: interpreters of cell-specific carbohydrate information during inflammation. Science 258:964–969.

Linn DM, Massey SC. 1992. GABA inhibits ACh release from the rabbit retina: A direct effect or feedback to bipolar cells? Vis Neurosci 8:97–106.

Masland RH. 1977. Maturation of function in the developing rabbit retina. J Comp Neurol 175:275–286.

Massey SC, Mills SL. 1996. A calbindin-immunoreactive cone bipolar cell type in the rabbit retina. J Comp Neurol 366:15–33.

Massey SC, Zhang J. 1998. A candidate for the blue/green ganglion cell in the rabbit retina. IOVS 39:S565.

McArdle CB, Dowling JE, Masland RH.1977. Development of outer segments and synapses in the rabbit retina. J Comp Neurol 175:253–274.

Mills SL, Massey SC. 1992. Morphology of bipolar cells labeled by DAPI in the rabbit retina. J Comp Neurol 321:133–149.

Negishi K, Kato S, Teranishi T. 1988. Dopamine cells and rod bipolar cells contain protein kinase C-like immunoreactivity in some vertebrate retinas. Neurosci Lett 94:247–252.

Nelson R, Famiglietti EV, Kolb H. 1978. Intracellular staining reveals different levels of stratification for on- and off-center ganglion cells in cat retina. J Neurophys 41:472–483.

Springer TA. 1994. Traffic signals for lymphocyte recirculation and leukocyte emigration: the multistep paradigm. Cell 76:301–314.

Strettoi E, Masland RH. 1995. The organization of the inner nuclear layer of the rabbit retina. J Neurosci 15:875–888.

Tauchi M, Masland RH. 1985. Local order among the dendrites of an amacrine cell population. J Neurosci 5:2494–2501.

Vaney DI. 1991. The mosaic of amacrine cells in the mammalian retina. Prog Retinal Res 9:49–100.

Vaney DI, Collin SP, Young HM. 1989. Dendritic relationships between cholinergic amacrine cells and direction-selective retinal ganglion cells. In: Weiler R, Osborne NN, editors. Neurobiology of the inner retina. Berlin: Springer-Verlag. p 157–168.

Wässle H, Riemann HJ. 1978. The mosaic of nerve cells in the mammalian retina. Proc R Soc Lond B 200:441–461.

Wright LL, MacQueen CL, Elston GN, Young HM, Pow DV, Vaney DI.1997. The DAPI-3 amacrine cells of the rabbit retina. Vis Neurosci 14:473–492.

Yang G, Masland RH. 1994. Receptive fields and dendritic structure of directionally selective retinal ganglion cells. J Neurosci 14:5267–5280.

Young HM, Vaney DI. 1991. Rod-signal interneurons in the rabbit: 1. rod bipolar cells. J Comp Neurol 310:139–153.